

# Massive MIMO with Cauchy Noise: Channel Estimation, Achievable Rate and Data Decoding

Ziya Gülgün, and Erik G. Larsson, *Fellow, IEEE*

**Abstract**—We consider massive multiple-input multiple-output (MIMO) systems in the presence of Cauchy noise. First, we focus on the channel estimation problem. In the standard massive MIMO setup, the users transmit orthonormal pilots during the training phase and the received signal at the base station is projected onto each pilot. This processing is optimum when the noise is Gaussian. We show that this processing is not optimal when the noise is Cauchy and as a remedy propose a channel estimation technique that operates on the raw received signal. Second, we derive uplink-downlink achievable rates in the presence of Cauchy noise for perfect and imperfect channel state information. Finally, we derive log-likelihood ratio expressions for soft bit detection for both uplink and downlink, and simulate coded bit-error-rate curves. In addition to this, we derive and compare the symbol detectors in the presence of both Gaussian and Cauchy noises. An important observation is that the detector constructed for Cauchy noise performs well with both Gaussian and Cauchy noises; on the other hand, the detector for Gaussian noise works poorly in the presence of Cauchy noise. That is, the Cauchy detector is robust against heavy-tailed noise, whereas the Gaussian detector is not.

**Index Terms**—Massive MIMO, Cauchy Noise, Achievable Rates, Symbol-error-rate (SER), Bit-error-rate (BER).

## I. INTRODUCTION

Massive multiple-input multiple-output (MIMO) is one of the core technologies in the 5G physical layer [2]. A massive MIMO base station (BS) is equipped with a large number of antennas (on the order of 100), each connected to an independent radio-frequency chain. Thanks to this flexibility, the BS can serve tens of users on the same time-frequency resources simultaneously. During the last decade, many aspects of massive MIMO technology have been investigated in depth, for example: power allocation and user association algorithms [3], hardware impairments [4].

This paper discusses an important aspect that has been largely ignored in the massive MIMO literature: the fact that noise and interference may not be Gaussian in general. More specifically, the noise can be impulsive and have a heavy-tailed distribution, corresponding to the presence of outliers. For example, in [5], impulsive noise was mentioned as one of the physical-layer challenges for 6G.

Z. Gülgün was with the Department of Electrical Engineering (ISY), 58183 Linköping, Sweden. He is now with Ericsson AB, 16440 Stockholm, Sweden (ziya.gulgün@ericsson.com).

E. G. Larsson is with the Department of Electrical Engineering (ISY), 58183 Linköping, Sweden e-mail: (erik.g.larsson@liu.se).

This work was supported by Security Link and the SURPRISE project funded by the Swedish Foundation for Strategic Research (SSF). A preliminary version of this paper was presented at the International Conference on Communications (ICC), 2022 [1].

## A. Motivation for Impulsive Noise

The Gaussian noise assumption is justified if the noise results from superposition of many independent components. However, this assumption does not apply in many real situations that may occur in electronic devices [6]. For example, in [7] the authors performed a series of measurements of electromagnetic noise for industrial wireless communications, and identified impulsive noise which can be modelled via Cauchy or Gamma distributions. Multi-carrier transmission with impulsive noise was studied in [8]–[10]. Adaptive demodulation for channels with impulsive noise was studied in [11]. Other examples are that ambient noise in shallow water for acoustic communication is highly impulsive [12]; the noise in powerline communication channels is impulsive [13]; interference in ad hoc networks can be impulsive [14]; and clutter models in radar signal processing are typically non-Gaussian [15]. Moreover, impulsive noise can also be generated by malicious transmitters (jammers).

One way to model impulsive noise is as symmetric  $\alpha$ -stable ( $S\alpha S$ ) random variables. The smaller  $\alpha$  is, the more impulsive the noise is. When  $\alpha$  is 1 and 2, the  $S\alpha S$  distribution becomes Cauchy and Gaussian, respectively. In the literature, impulsive noise ( $S\alpha S$ ) has been studied in various contexts. For example, array signal processing with impulsive noise is treated in [16], [17]. Spectrum sensing with  $S\alpha S$  channel was studied in [18]. Localization problems in the presence of  $\alpha$ -stable noise were investigated in [19]. The probability density functions (pdfs) of  $S\alpha S$  distributions are approximated and the signal detection performances of these pdfs are investigated in [20]. In [21], soft-decision metrics for coded signals in Cauchy noise were derived. An interesting conclusion in [21] is that the performance loss of the detector designed for Cauchy noise when exposed to Gaussian noise is much smaller than the loss when the detector designed for Gaussian noise is exposed to Cauchy noise. Indeed, the detector designed for Gaussian noise works poorly in the presence of Cauchy noise, whereas the detector designed for Cauchy noise is very robust to the actual distribution of the noise.

We consider massive MIMO specifically with Cauchy ( $S(\alpha = 1)S$ ) noise. Another paper that addressed channel estimation for massive MIMO with impulsive noise is [22]. The impulsive noise in [22] is modelled as a mixture of Gaussian noise and outliers, rather than via an  $S\alpha S$  distribution; the mixture weights (probabilities of outliers) are estimated by tuning a sparsity level parameter. In contrast to [22], we chose to work with Cauchy noise since it is simpler to deal with analytically (for example, the Cauchy distribution is preserved under linear combinations) and it has fewer parameters that

require tuning to the impulsive level of the noise. In addition, compared with [22], we provide achievable rate expressions and soft decoding metrics.

### B. Summary of Technical Contributions and Organization of the Paper

We describe a system model for single-cell massive MIMO with Cauchy noise and focus on the channel estimation in Section II where we derive two types of channel estimators. In the first, the received signal at the base station (BS) is de-spread by correlating it with each user's pilot signal. In the presence of Gaussian noise, this entails no loss of information; the de-spread received pilots are sufficient statistics. However, this is not the case if the noise is non-Gaussian. The second channel estimation approach rather estimates the channels from the raw received signal without de-spread first, and is shown to be superior. Next, in Section III, we derive uplink and downlink achievable rate expressions for the cases of perfect and imperfect channel state information (CSI). Thereby, for the imperfect CSI case, the channel estimates are used as side information. In Section IV, we then derive log-likelihood ratio (LLR) expressions for soft decoding both for uplink and downlink. Finally, in Section V we give numerical results on achievable rates and bit-error-rate (BER) for the different detectors.

This paper is a comprehensive extension of our conference paper [1]. The new material compared to [1] is mainly that (i) we analyze achievable rates for both perfect and imperfect CSI, (ii) we analyze the decoding performance of a Cauchy receiver in the presence of noise with other  $S\alpha S$  distributions, (iii) we derive LLR expressions for soft decoding, and (iv) we present numerical results on achievable rates and coded BER.

### C. Notation

$|\cdot|$ ,  $(\cdot)^T$ ,  $(\cdot)^*$  and  $(\cdot)^H$  denote the absolute value of a scalar, determinant of a matrix, transpose, conjugate and conjugate transpose operators, respectively. Boldface lowercase letters,  $\mathbf{x}$ , denote column vectors, boldface uppercase letters,  $\mathbf{X}$ , denote matrices, and uppercase letters,  $X$ , denote random variables. The  $l_p$  norm is denoted by  $\|\mathbf{x}\|_p$ .  $\mathbb{E}[\cdot]$  refers to the expectation operator.  $\Re(\cdot)$  is the real part of a complex number.

## II. SYSTEM MODEL AND CHANNEL ESTIMATION

### A. System Model

We consider a single-cell massive MIMO system including a BS equipped with  $M$  antennas, serving  $K$  users where each user has a single antenna. A block-fading model is considered in which the channel is constant and frequency-flat in a coherence block with size  $T$  samples. A sub-block with length  $\tau$  is reserved for the channel estimation and the rest of the coherence block with length  $T - \tau$  is dedicated to data transmission.

During the training phase, the users transmit orthonormal pilot vectors with length  $\tau$  to the BS.  $\tau$  should be greater than or equal to  $K$  and less than  $T$ . Let us denote the pilot vector for the  $k^{\text{th}}$  user by  $\phi_k \in \mathbb{C}^\tau$ . Since these vectors are

orthonormal,  $\|\phi_k\|^2 = 1$  and  $\phi_k^H \phi_j = 0$  for  $k \neq j$ . It remains an open question under what exact circumstances orthogonal pilot sequences are optimal in the presence of Cauchy noise. (For example, in Cauchy noise, unlike in Gaussian noise, de-spreading is suboptimal; see Section II-B.) The choice of orthogonal pilots, however, is optimal for Gaussian noise and it is the standard design choice most systems; hence, we adopt it here. Even when restricting the pilots coming from an orthogonal pilot book, numerical evidence shows that the performance is different for different choices of this pilot book (unlike in the Gaussian case). For example, pilots chosen from the identity matrix and pilots chosen from a normalized discrete Fourier transform (DFT) matrix do not provide the same performances. In this work, we choose the pilots from the normalized DFT matrix because this increases the number of observed realizations in the receiver side, which is important because of the outliers in the Cauchy distribution.

The received pilot signal in the BS can be expressed as:

$$\mathbf{Y} = \sum_{k=1}^K \sqrt{\tau p_k} \mathbf{h}_k \phi_k^T + \mathbf{N}, \quad (1)$$

where  $p_k$  is the power of the received signal corresponding to the  $k^{\text{th}}$  user, and  $\mathbf{h}_k \in \mathbb{C}^M$  is the  $k^{\text{th}}$  user's channel vector. The elements in all channel vectors are independent, identically distributed (i.i.d.) circularly symmetric complex Gaussian random variables, i.e.,  $\mathbf{h}_k \sim \mathcal{CN}(0, \mathbf{I})$ , and  $\mathbb{E}\{\mathbf{h}_k^H \mathbf{h}_m\} = 0$  for  $k \neq m$ , corresponding to uncorrelated Rayleigh fading.  $\mathbf{N}$  is an  $M \times \tau$  noise matrix containing i.i.d. isotropic complex Cauchy random variables with dispersion parameter  $\gamma = 1$ . If the noise components were complex Gaussian with unit variance,  $p_k$  would have the meaning of signal-to-noise ratio (SNR). However, it is not meaningful to define  $p_k$  as SNR with Cauchy noise, because the second-order moment of the Cauchy distribution is infinite; see Appendix A. Therefore, we use the term signal-to-dispersion ratio (SDR) for  $p_k$  in this work.

To contrast SDR and SNR, we investigate the relation between the standard deviation of the Gaussian distribution and the dispersion of the Cauchy distribution. For the (real-valued) Gaussian distribution, the probability that a realization,  $X$ , lies between  $-\sigma$  and  $\sigma$ , where  $\sigma$  is the standard deviation, is around 2/3. The probability that a (real-valued) Cauchy realization,  $X$ , lies between 0 (the median) and  $t$  can be expressed as:

$$P(0 < X < t) = \frac{1}{\pi} \tan^{-1} \left( \frac{t}{\gamma} \right), \quad (2)$$

where  $\gamma$  is the dispersion. From (2), we infer that the probability that a Cauchy realization,  $X$ , lies between  $-1.7\gamma$  and  $1.7\gamma$  is around 2/3. Therefore, if we set  $\sigma = 1.7\gamma$ , the probability is 2/3 for both a Gaussian and a Cauchy random variable.

### B. Channel Estimation

In this section, we propose two channel estimation techniques for the case when Cauchy noise is present. The first relies on de-spreading of the received pilots. The second, in contrast, operates on the original received pilots in (1) without performing de-spreading.

1) *Channel Estimation with De-spreading Operation*: After the de-spreading operation, the signal corresponding to the  $k^{\text{th}}$  user can be expressed as:

$$\mathbf{y}_k = \mathbf{Y} \phi_k^* = \sqrt{\tau p_k} \mathbf{h}_k + \mathbf{n}_k, \quad (3)$$

where  $\mathbf{n}_k = \mathbf{N} \phi_k^*$ . Now, let us analyze the statistic of  $\mathbf{n}_k$ .

**Proposition 1.**  $\mathbf{n}_k$  contains i.i.d. isotropic complex Cauchy random variables with the dispersion  $\gamma'_k = \gamma \|\phi_k\|_1 = \gamma \sum_{i=1}^{\tau} |\phi_k[i]|$  where  $\phi_k[i]$  is the  $i^{\text{th}}$  element of  $\phi_k$ .

*Proof*: First, since the row vectors in  $\mathbf{N}$  are independent, the elements in  $\mathbf{n}_k$  are mutually independent.

Next, as a preliminary observation that we will exploit in the proof, we analyze the statistics of  $cX$  where  $c \in \mathbb{C}$  and  $X$  is an isotropic complex Cauchy random variable. By using (52), we can express the characteristic function of  $cX$  as:

$$\phi_{(cX)}(\omega) = \mathbb{E}[\exp(j\Re(\omega(cX)^*))] = \mathbb{E}[\exp(j\Re(c^* \omega X^*))]. \quad (4)$$

Let us define  $\omega' = c^* \omega$ . Then (4) can be rewritten as:

$$\mathbb{E}[\exp(j\Re(\omega' X^*))] = \exp(-\gamma|\omega'|) = \exp(-\gamma|c|\omega). \quad (5)$$

Now, we focus on the  $l^{\text{th}}$  element in  $\mathbf{n}_k$ , denoted as  $\mathbf{n}_k[l]$ . The characteristic function of  $\mathbf{n}_k[l]$  is:

$$\phi_{\mathbf{n}_k[l]}(\omega) = \mathbb{E}[\exp(j\Re(\omega(\mathbf{n}_k[l])^*))] \quad (6a)$$

$$= \mathbb{E} \left[ \exp \left( j\Re \left( \omega \sum_{i=1}^{\tau} \phi_k[i] \mathbf{N}[l, i]^* \right) \right) \right] \quad (6b)$$

$$= \prod_{i=1}^{\tau} \mathbb{E}[\exp(j\Re(\omega \phi_k[i] \mathbf{N}[l, i]^*))], \quad (6c)$$

where (6b) can be represented as a product of random variables as in (6c) because all random variables are mutually independent ( $\mathbf{N}[l, i]$  is the element in the  $l^{\text{th}}$  row and the  $i^{\text{th}}$  column of  $\mathbf{N}$  and  $\mathbf{N}$  contains i.i.d. random variables). By using (5), the following is obtained:

$$\begin{aligned} \phi_{\mathbf{n}_k[l]}(\omega) &= \prod_{i=1}^{\tau} \mathbb{E}[\exp(j\Re(\omega \phi_k[i] \mathbf{N}[l, i]^*))] \quad (7) \\ &= \prod_{i=1}^{\tau} \exp(-\gamma|\phi_k[i]||\omega|) \\ &= \exp \left( -\gamma \sum_{i=1}^{\tau} |\phi_k[i]| |\omega| \right), \end{aligned}$$

which concludes the proof. ■

Proposition 1 presents an important result. Although the de-spreading operation preserves the distribution of noise, the dispersion may increase. For example, if the pilot signals are chosen from a normalized DFT matrix, the dispersion after de-spreading operation becomes  $\gamma'_k = \gamma \sqrt{\tau} \forall k$ . This is not the case for the isotropic complex Gaussian noise because a multiplication with a unitary matrix does not change the noise variance [23, Chapter 3].

Now, we need to estimate the channels from (3). Most existing papers use minimum mean-square-error (MMSE) or linear MMSE techniques to estimate the channels [23], [24].

However, these techniques cannot be applied in the presence of Cauchy noise because the first and second order moments for this noise distribution are undefined. Therefore, here we take a maximum-likelihood (ML) approach. The maximum-a-posteriori (MAP) technique could also be applied if a prior on the channel statistic is known. The difference between MAP and ML is that the pdf of channel statistic appears in the objective function; in this paper, we only consider ML for simplicity.

From (3), the likelihood function for  $\mathbf{h}_k$  based on the de-spread data is

$$p(\mathbf{y}_k | \mathbf{h}_k) = \prod_{i=1}^M \frac{\gamma'_k}{2\pi((\gamma'_k)^2 + |\mathbf{y}_k[i] - \sqrt{\tau p_k} \mathbf{h}_k[i]|^2)^{3/2}}. \quad (8)$$

Based on (8), the ML estimate of the channel  $\mathbf{h}_k$  is:

$$\hat{\mathbf{h}}_k^{\text{ML}} = \arg \max_{\mathbf{h}_k} p(\mathbf{y}_k | \mathbf{h}_k) = \frac{\mathbf{y}_k}{\sqrt{\tau p_k}}. \quad (9)$$

From (3) and (9), it can be immediately seen that  $\hat{\mathbf{h}}_k^{\text{ML}}$  is also identical with the least-squares channel estimate for  $\mathbf{h}_k$ .

Next, we analyze whether  $\mathbf{y}_k$  is a sufficient statistic or not. To do this, we go back the unprocessed received signal in (1). The likelihood function based on the raw data in (1) is:

$$\begin{aligned} p(\mathbf{Y} | \mathbf{h}_1, \dots, \mathbf{h}_K) &= \quad (10) \\ &= \prod_{l=1}^M \prod_{i=1}^{\tau} \frac{\gamma}{2\pi \left( \gamma^2 + |\mathbf{Y}[l, i] - \sum_{k=1}^K \sqrt{\tau p_k} \mathbf{h}_k[l] \phi_k[i]|^2 \right)^{3/2}}, \end{aligned}$$

where  $\mathbf{Y}[l, i]$  is the element in the  $l^{\text{th}}$  row and  $i^{\text{th}}$  column of  $\mathbf{Y}$ . In order to obtain a sufficient statistic, there should exist a factorization of the likelihood function in (10) as [25, Chapter 4]:

$$p(\mathbf{Y} | \mathbf{h}_1, \dots, \mathbf{h}_K) = h(\mathbf{Y})g(T(\mathbf{Y}), \mathbf{h}_1, \dots, \mathbf{h}_K), \quad (11)$$

where  $g(\cdot)$  and  $h(\cdot)$  are some functions, and  $T(\cdot)$  is the sufficient statistic. Note that  $g(\cdot)$  should depend on  $\mathbf{Y}$  only through  $T(\mathbf{Y})$ . Because of the fractional exponent  $3/2$  in the denominator, one cannot expand the corresponding term. One can multiply the all the terms under the fractional exponent  $3/2$  but a function  $T(\cdot)$  cannot be obtained because of the many cross-terms that appear.

*Remark 1*: Let us consider an affine estimator of the  $k^{\text{th}}$  user's channel which has the structure  $\mathbf{Y} \mathbf{a}_k + \mathbf{b}_k$  where  $\mathbf{Y} \mathbf{a}_k \neq 0$ ,  $\mathbf{a}_k \in \mathbb{C}^{\tau}$  and  $\mathbf{b}_k \in \mathbb{C}^M$ . As a result of Proposition 1, this affine estimator can be linearly decomposed into noise which has a complex isotropic Cauchy distribution and a signal part. For example, from (3),  $\mathbf{n}_k$  is the additive part of  $\mathbf{y}_k$  which has the complex isotropic Cauchy distribution. Therefore, the mean of  $\mathbf{y}_k$  is undefined and the variance of  $\mathbf{y}_k$  is infinite for the affine estimators.

2) *Channel Estimation from the Unprocessed Received Signal*: In this section, we derive the ML estimates for the channel vectors based on the unprocessed received signal in (1). The likelihood function is given in (10). Maximizing (10) is very complicated because the parameters of all users interact with each other. To solve this problem, one approach is to use a coordinate search algorithm [26, Chapter 9]. The idea is

as follows: First, assign some initial values to all parameters except  $\mathbf{h}_1$ . Then find the estimate of  $\mathbf{h}_1$  that maximizes the likelihood function. Next, with the so-obtained value of  $\mathbf{h}_1$ , find the estimate of  $\mathbf{h}_2$  that maximizes the likelihood function and so forth. One can then iteratively loop through all  $\mathbf{h}_k$  and then return to  $\mathbf{h}_1$ , and run another complete iteration over all  $k$ . This procedure goes on until there is a sufficiently small difference between the norms of the channel estimates in the current round compared to in the previous round.

The coordinate descent algorithm guarantees that the function value obtained in an iteration is less than or equal to the function value obtained in the previous iteration. However, the algorithm may converge to a non-stationary point, or the algorithm can continue searching infinitely many times for non-convex functions [27]. The examples in [27] are very special examples, but the conclusions therein prevent us from making a general statement that the algorithm converges to a stationary point. Bertsekas [28] shows in Proposition 2.7.4 that if the objective is continuously differentiable, i.e., the first derivative is continuous, and the minimizer along any coordinate direction from any point is unique, then the algorithm converges to a stationary point. The objective function in (10) is continuously differentiable, but we do not have proof that the minimizer along any direction is not unique. (In [1], we claimed that the coordinate descent algorithm converges to a locally optimum point, but this is unknown.) Numerical experiments suggest that the convergence to a stationary point depends on the initial point.

In the first iteration, we assign  $\hat{\mathbf{h}}_k^{\text{ML}}$  in (9) to  $\mathbf{h}_k$  for  $k = 2, \dots, K$  as initial solutions. This results in the modified objective function in (10) for  $\mathbf{h}_1$  as follows:

$$p(\mathbf{Y}'|\mathbf{h}_1) = \prod_{l=1}^M \prod_{i=1}^{\tau} \frac{\gamma}{2\pi (\gamma^2 + |\mathbf{Y}'[l, i] - \sqrt{\tau p_1} \mathbf{h}_1[l] \phi_1[i]|^2)^{3/2}}, \quad (12)$$

where

$$\mathbf{Y}' = \mathbf{Y} - \sum_{k=2}^K \sqrt{\tau p_k} \hat{\mathbf{h}}_k^{\text{ML}} \phi_k^T.$$

When maximizing with respect to the first element of  $\mathbf{h}_1$ , we have  $M$  separable maximization problems. The corresponding observation vector is the first row from  $\mathbf{Y}'$ . Therefore, we need to maximize the following:

$$\prod_{i=1}^{\tau} \frac{\gamma}{2\pi (\gamma^2 + |\mathbf{Y}'[1, i] - \sqrt{\tau p_1} \mathbf{h}_1[1] \phi_1[i]|^2)^{3/2}}. \quad (13)$$

Taking the logarithm, the maximization of (13) is equivalent to the minimization of the following:

$$\sum_{i=1}^{\tau} \log (\gamma^2 + |\mathbf{Y}'[1, i] - \sqrt{\tau p_1} \mathbf{h}_1[1] \phi_1[i]|^2). \quad (14)$$

To minimize (14), we use the gradient descent algorithm [26, Chapter 3] and give the details in Appendix B. Note that the function in (14) is nonconvex because the Cauchy distribution is non-log-convex.

*Remark 2:* Suppose we want to estimate a parameter from data containing Cauchy noise. The estimate may have a certain variance and even the Cramer-Rao bound may exist for the

estimate [19]. In general, when the noise is Cauchy, the relation between the ML estimate and the observed data is not affine, not even for a linear signal model. Hence, the ML estimate may have a certain variance, although sometimes it does not; for example, see (9).

### III. ACHIEVABLE RATES WITH CAUCHY NOISE

In this section, we present the uplink and downlink achievable rates for the massive MIMO communication link with perfect and imperfect CSI. In the literature, [29] derived the capacity for the scalar Cauchy channel under a logarithmic constraint on the input distribution; see [29] for details. Another paper [30] derived some capacity bounds for S $\alpha$ S noise channel with  $\alpha > 1$  which does not cover the Cauchy noise. As the exact capacity appears intractable for our setup when the noise is Cauchy, in this paper we focus on achievable rates (lower bounds on capacity). To study the effects of the Cauchy noise specifically, we restrict this analysis to the one-user scenario.

#### A. The Uplink Achievable Rate

The mutual information of the single-input single-output (SISO) channel can be calculated empirically; see details in Appendix C. Now we apply this result to the case of a single-input multiple-output channel with Cauchy noise. We start with the perfect CSI case. Mathematically, we can express the received signal as an  $M$ -vector:

$$\mathbf{y} = \sqrt{p^{\text{ul}}} \mathbf{h} \mathbf{x} + \mathbf{n}, \quad (15)$$

where  $p^{\text{ul}}$  is the uplink SDR,  $x$  is the transmitted signal,  $\mathbf{h} \in \mathbb{C}^M$  is the channel gain. Both the channel gain and its statistics are known by the receiver.  $\mathbf{n} \in \mathbb{C}^M$  is the noise vector including complex isotropic Cauchy random variables with unit dispersion parameter. Let us define a joint random variable  $\bar{Y} = [Y_1, \dots, Y_M]^T$  comprising the random variables observed at each antenna and a joint random variable  $\bar{H} = [H_1, \dots, H_M]^T$  including the channel realizations known by the receiver. Assume that the transmitted signal is chosen uniformly from the discrete set  $A_X$  with cardinality  $S$ . After this, we can define the uplink achievable rate:

$$R^{\text{ul}} = \log_2 S - \mathbb{E}_{X, \bar{Y}, \bar{H}} \left\{ \log_2 \left( \frac{\sum_{x \in A_X} p(\bar{Y}, \bar{H}|x)}{p(\bar{Y}, \bar{H}|X)} \right) \right\}. \quad (16)$$

All  $(Y_i, H_i)$  pairs are independent to each other if  $X$  is given. Hence, (16) can be rewritten as:

$$R^{ul} = \log_2 S - \mathbb{E}_{X, \bar{Y}, \bar{H}} \left\{ \log_2 \left( \frac{\sum_{x \in A_X} \prod_{i=1}^M p(Y_i, H_i | x)}{\prod_{i=1}^M p(Y_i, H_i | X)} \right) \right\} \quad (17)$$

$$= \log_2 S - \mathbb{E}_{X, \bar{Y}, \bar{H}} \left\{ \log_2 \left( \frac{\sum_{x \in A_X} \prod_{i=1}^M p(Y_i | H_i, x)}{\prod_{i=1}^M p(Y_i | H_i, X)} \right) \right\},$$

where  $p(y_i | h_i, x)$  is:

$$p(y_i | x) = \frac{\gamma}{2\pi(\gamma^2 + |y_i - \sqrt{p^{ul}} h_i x|^2)^{3/2}}, \quad (18)$$

where  $y_i$  and  $h_i$  are the  $i^{th}$  elements of  $\mathbf{y}$  and  $\mathbf{h}$ , respectively.

Now consider the imperfect CSI case. The BS estimates the channel denoted by  $\hat{\mathbf{h}}$  in the training phase. These estimates are used as side information to calculate achievable rates. This calculation exploits standard results on capacity bounding with side information; for example, see [23, Sec. 2.3]. Since there exists an error between the estimates and the real channels, the achievable rates for the imperfect CSI case are less than or equal to the achievable rates for the perfect CSI case [31].

Let us define a joint random variable  $\hat{H} = [\hat{H}_1, \dots, \hat{H}_M]^T$  including the random variables that represent the channel estimates. Then, the uplink achievable rate for the imperfect CSI case can be expressed as:

$$R^{ul, \text{imCSI}} = \left(1 - \frac{\tau}{T}\right) \times \left( \log_2 S - \mathbb{E}_{X, \bar{Y}, \hat{H}} \left\{ \log_2 \left( \frac{\sum_{x \in A_X} \prod_{i=1}^M p(Y_i | x, H_i = \hat{H}_i)}{\prod_{i=1}^M p(Y_i | X, H_i = \hat{H}_i)} \right) \right\} \right), \quad (19)$$

where  $p(y_i | x, h_i = \hat{h}_i)$  can be obtained from (18) when  $h_i = \hat{h}_i$ . The pre-log factor appears in (19) because we do not send any data during  $\tau$  samples of each coherence block.

It is important to note that we do not have the statistics of the channel estimation error, because we do not have closed-form channel estimates. However, for the uplink the BS can calculate some statistics of the channel estimation error empirically. In IV-C, we explain how the BS calculates the statistics of the channel estimation error and how the effects of this estimation error can be considered as additional noise term.

*Remark 3:* Let us define a variable  $y = \mathbf{v}^H \mathbf{y}$ , where  $\mathbf{v}$  is a decoding vector. For the perfect CSI and the Gaussian cases, we do not lose any information if  $\mathbf{v} = \mathbf{h} / \|\mathbf{h}\|$  [32]. In other words,  $y$  is a sufficient statistic for  $\mathbf{y}$ . However this is not the case in Cauchy noise. Therefore, we derive the rate expressions by using  $y$  for perfect and imperfect CSI.

## B. The Downlink Achievable Rate

Now we find the achievable rate of a communication link where the BS transmits the data to the user. Again, we start with the perfect CSI case. The received signal can be written as,

$$y = \sqrt{p^{dl}} \mathbf{h}^T \mathbf{a} x + n, \quad (20)$$

where  $p^{dl}$  is the downlink SDR,  $x$  is the transmitted signal,  $\mathbf{h} \in \mathbb{C}^M$  is the channel gain that is known by the receiver,  $\mathbf{a} \in \mathbb{C}^M$  is the precoder vector designed by the BS,  $n$  is the Cauchy noise with unit dispersion parameter. We assume that  $\|\mathbf{a}\|_2 = 1$  so that we do not obtain any power gain from the precoder. To maximize the received useful signal power,  $\mathbf{a}$  should equal  $\mathbf{h}^* / \|\mathbf{h}\|$ . Hence, the downlink achievable rate becomes:

$$R^{dl} = \log_2 S - \mathbb{E}_{X, Y} \left\{ \log_2 \left( \frac{\sum_{x \in A_X} p(Y|x)}{p(Y|X)} \right) \right\}, \quad (21)$$

where  $p(y|x)$  is:

$$p(y|x) = \frac{\gamma}{2\pi(\gamma^2 + |y - \sqrt{p^{dl}} \|\mathbf{h}\|_2 x|^2)^{3/2}}. \quad (22)$$

Similar to the uplink achievable rates, we use the channel estimates as side information to calculate the downlink achievable rates. To do this, the precoder vector should be  $\hat{\mathbf{h}}^*$  for the imperfect CSI case. Let us define a joint random variable  $\bar{H} = [H_1, \dots, H_M]^T$ . The achievable rate is given by:

$$R^{dl, \text{imCSI}} = \left(1 - \frac{\tau}{T}\right) \times \left( \log_2 S - \mathbb{E}_{X, Y, \hat{H}} \left\{ \log_2 \left( \frac{\sum_{x \in A_X} p(Y|x, \bar{H} = \hat{H})}{p(Y|X, \bar{H} = \hat{H})} \right) \right\} \right), \quad (23)$$

where  $p(y|x, \mathbf{h} = \hat{\mathbf{h}})$  can be obtained from (22) when  $\mathbf{h} = \hat{\mathbf{h}}$ .

In the downlink, the effect of the channel estimation error is implicit, entering only via the precoder vector, but not explicitly visible in the achievable rate expression.

*Remark 4:* For the Gaussian noise and perfect CSI case, we observe the uplink-downlink duality when the maximum-ratio (MR) decoder and MR precoder are used in the uplink and downlink, respectively. Therefore, we have the same achievable rates. However, this appears not to be the case with Cauchy noise, because linear processing of the received signal in the uplink is suboptimal.

## C. The Cauchy Decoder with Other S $\alpha$ S Noise

In this section, we evaluate the performance of the Cauchy decoder in the presence of other complex isotropic S $\alpha$ S noise. We focus on complex isotropic S $\alpha$ S noise with  $1 < \alpha < 2$ , for which capacity bounds exist in closed form [30].

For the complex isotropic S $\alpha$ S noise with  $1 < \alpha < 2$ , the pdf can be expressed as [33, Chapter 3]:

$$f_X(x) = \frac{1}{\pi \alpha \gamma^{2/\alpha}} \sum_{k=0}^{\infty} \frac{(-1)^k}{2^{2k+1} (k!)^2} \Gamma\left(\frac{2k+2}{\alpha}\right) \left(\frac{|x|}{\gamma^{1/\alpha}}\right)^{2k}, \quad (24)$$

where  $\Gamma(\cdot)$  is the standard Gamma function. The pdf in (24) is not in closed-form. Therefore, to develop a decoding metric, either this pdf would have to be approximated, or implemented via a table lookup. We consider that the Cauchy decoding metric is used, and next evaluate how it performs when it is exposed to noise with a  $S(1 < \alpha \leq 2)S$  distribution.

Consider a SISO channel:

$$y = \sqrt{p}x + n, \quad (25)$$

where  $y$ ,  $x$  and  $p$  are the received signal, transmitted signal and the received power, respectively. Let us assume that  $\mathbb{E}[|X^R|] = \mathbb{E}[|X^I|]$ . The capacity bounds presented in Eq. (3) of [30] apply for the case of real-valued  $S\alpha S$  distributions. For complex  $S(1 < \alpha \leq 2)S$ , the real and imaginary parts are statistically dependent, which means that the capacity *at least* doubles when considering the real and imaginary parts of the channel together. This results in the bound:

$$C \geq \frac{2}{\alpha} \log_2 \left( 1 + \left( \frac{\sqrt{p}c}{\mathbb{E}[|N^R|]} \right)^\alpha \right), \quad \mathbb{E}[|X^R|] \leq c, \quad (26)$$

where  $C$  is the capacity for (25), and  $N^R$  is the real part of noise having the  $S\alpha S$  distribution for the real-valued realizations. Note that  $N^R$  is identically distributed with the imaginary part. The fractional moment of  $N^R$  can be expressed as [33, Chapter 3]:

$$\mathbb{E}[|N^R|^p] = \gamma^{p/\alpha} \frac{2^{p+1} \Gamma(\frac{p+1}{2}) \Gamma(-\frac{p}{\alpha})}{\alpha \sqrt{\pi} \Gamma(-\frac{p}{2})}, \quad 0 < p < \alpha. \quad (27)$$

Now, assume that  $y$  in (25) is decoded by using the Cauchy model. This decoding technique is called *mismatched decoding* because the actual present noise has different statistics than what the decoder assumes [34]. The achievable rate obtained from the mismatched decoder is called as *mismatched achievable rate*. The mismatched achievable rate is a lower bound on the actual mutual information [35, eq. (34)] so for the capacity:

$$C \geq I(X; Y) \geq \log_2 S - \mathbb{E}_{X,Y} \left\{ \log_2 \frac{\sum_{x \in A_X} \tilde{p}(Y|x)}{\tilde{p}(Y|X)} \right\}, \quad (28)$$

where  $\tilde{p}(y|x)$  is the decoder metric that is assumed to be Cauchy model.

In Section V, we compare the capacity bound in (26) and the mismatched achievable rate in (28).

#### IV. DATA DECODING

In this section, we present hard decision metrics for uncoded symbol detection and soft decision metrics for coded bit detection, respectively. For the hard symbol detection, we only consider the uplink for both Gaussian and Cauchy noises. For the soft bit detection, we consider the uplink and the downlink for Cauchy case only.

##### A. Symbol Detection for The Uplink (Uncoded Modulation)

In this section, we use the channel estimates obtained in Section II-B to infer the transmitted data. Express the received signal as:

$$\mathbf{r} = \sum_{k=1}^K \sqrt{p_k} \mathbf{h}_k s_k + \mathbf{n}, \quad (29)$$

where  $s_k$  is the symbol transmitted by user  $k$ , chosen from a certain alphabet. If the noise is Gaussian, the detector will be:

$$\hat{\mathbf{s}} = \arg \min_{\mathbf{s}} \sum_{i=1}^M \left| \mathbf{r}[i] - \sum_{k=1}^K \sqrt{p_k} \hat{\mathbf{h}}_k [i] s_k \right|^2. \quad (30)$$

For the case of Cauchy noise in  $\mathbf{n}$ , we insert the channel estimates into the likelihood function associated with (29):

$$p(\mathbf{r} | \hat{\mathbf{h}}_1, \dots, \hat{\mathbf{h}}_K, \mathbf{s}) = \prod_{i=1}^M \frac{\gamma}{2\pi \left( \gamma^2 + \left| \mathbf{r}[i] - \sum_{k=1}^K \sqrt{p_k} \hat{\mathbf{h}}_k [i] s_k \right|^2 \right)^{3/2}}, \quad (31)$$

where  $\mathbf{s} = [s_1 \dots s_K]^T$ . Therefore the ML estimates of the symbols are:

$$\hat{\mathbf{s}} = \arg \min_{\mathbf{s}} \sum_{i=1}^M \log \left( \gamma^2 + \left| \mathbf{r}[i] - \sum_{k=1}^K \sqrt{p_k} \hat{\mathbf{h}}_k [i] s_k \right|^2 \right). \quad (32)$$

The problems in (30) and (32) are constellation-constrained minimization problems. Neglecting the constellation constraint, the solution of the problem in (30) is the well-known zero-forcing (ZF) detector:

$$\hat{\mathbf{s}} = (\hat{\mathbf{H}}^H \hat{\mathbf{H}})^{-1} \hat{\mathbf{H}}^H \mathbf{r}, \quad (33)$$

where  $\hat{\mathbf{H}} \in \mathbb{C}^{M \times K}$  is a matrix where the  $k^{th}$  column is  $\hat{\mathbf{h}}_k$ .

For the problem with Cauchy noise, (32), again we neglect the constellation constraint and obtain a soft decision for each symbol from the alphabet by evaluating the minimum Euclidean distance. The problem in (32) can be solved by using the gradient descent algorithm that is described in Section II-B2. For the initial solution of  $\hat{\mathbf{s}}$  in the gradient descent, we take the zero vector.

Note that the problem in (32) has more than one local optimum solution. The global solution of (30), however, is unique and easily given by the ZF.

##### B. Soft Decision Metric for The Uplink (Coded Modulation)

Consider again the received signal in (29). We now focus on the LLR expression for the  $i^{th}$  bit of the  $k^{th}$  symbol. This LLR can be written as:

$$l_{k,i} = \log \left( \frac{p(b_{k,i} = 0 | \mathbf{r})}{p(b_{k,i} = 1 | \mathbf{r})} \right) = \log \left( \frac{\sum_{\mathbf{s}: b_{k,i}(\mathbf{s})=0} p(\mathbf{r} | \mathbf{s}) p(\mathbf{s})}{\sum_{\mathbf{s}: b_{k,i}(\mathbf{s})=1} p(\mathbf{r} | \mathbf{s}) p(\mathbf{s})} \right). \quad (34)$$

The notation  $\mathbf{s} : b_{k,i}(\mathbf{s}) = \beta$  represents that the set contains all  $\mathbf{s}$  where  $b_{k,i}$  is equal to  $\beta$ . Without loss of generality, we assume that  $p(\mathbf{s})$  equals  $1/S^K$ , where  $S$  is the cardinality of the symbol alphabet. The BS makes use of the channel estimates as the real channels. Therefore  $p(\mathbf{r} | \mathbf{s})$  is the same as (31).

The complexity of (34) is huge because of the many terms in the summation. To simplify the expression in (34), one approach is to replace the summation with the largest term; this is called the *max-log* approximation [36]. However, it has still

high complexity because we need to search through  $\frac{S}{2} \times S^{K-1}$  candidates just for one bit. Therefore, finding the largest term may be infeasible. Instead, we propose the following:

- For the  $k^{\text{th}}$  symbol, there are  $S/2$  symbols whose  $i^{\text{th}}$  bit is 0. Let us denote these symbols by  $S_k^{i=0} = \{s_{k,1}^{i=0}, \dots, s_{k,S/2}^{i=0}\}$ . For each  $S/2$  symbol, we can solve the following maximization problem by neglecting the constellation constraint:

$$\tilde{\mathbf{s}}_{k,t}^{i=0} = \arg \max_{\tilde{\mathbf{s}}} p(\mathbf{r} | \tilde{\mathbf{s}}, s_k^{i=0} = s_{k,t}^{i=0}), \quad (35)$$

where  $t$  ranges from 1 to  $S/2$ ,  $\tilde{\mathbf{s}}_{k,t}^{i=0}$  is an  $(K-1) \times 1$  vector including soft estimates when  $s_k^{i=0} = s_{k,t}^{i=0}$ . By combining (32) and (35), the problem in (35) is equivalent to:

$$\begin{aligned} \tilde{\mathbf{s}}_{k,t}^{i=0} = \arg \min_{\tilde{\mathbf{s}}} \sum_{i=1}^M \log \left( \gamma^2 + \left| \mathbf{r}[i] - \sqrt{p_k} \hat{\mathbf{h}}_k[i] s_{k,t}^{i=0} \right. \right. \\ \left. \left. - \sum_{n=1, n \neq k}^K \sqrt{p_n} \hat{\mathbf{h}}_n[i] \tilde{s}_n \right|^2 \right). \end{aligned} \quad (36)$$

We can obtain hard estimates from  $\tilde{\mathbf{s}}_{k,t}^{i=0}$  based on the Euclidean distance between soft estimates and the real symbols. Let us denote  $\hat{\mathbf{s}}_{k,t}^{i=0}$  a vector including the hard estimates.

- Choose the maximum among the  $S/2$  likelihood terms. The LLR is approximately equal to:

$$\begin{aligned} l_{k,i} \approx \log \left( \max_{\{\hat{\mathbf{s}}_{k,t}^{i=0}\}_{t=1}^{S/2}} p(\mathbf{r} | \hat{\mathbf{s}}_{k,t}^{i=0}, s_k^{i=0} = s_{k,t}^{i=0}) \right) - \\ \log \left( \max_{\{\hat{\mathbf{s}}_{k,t}^{i=1}\}_{t=1}^{S/2}} p(\mathbf{r} | \hat{\mathbf{s}}_{k,t}^{i=1}, s_k^{i=1} = s_{k,t}^{i=1}) \right) \end{aligned} \quad (37)$$

- By doing so, we need to solve  $S/2$  optimization problems for each bit. In order to obtain the gradient for (36), we need  $\mathcal{O}(MK^2)$  flops. Unlike our proposed method, the complexity of max-log approximation, which is  $S/2 \times S^{K-1}$ , grows with  $K$  exponentially.

### C. Soft Decision Metric for The Uplink Including Channel Estimation Error (Coded Modulation)

In this section we consider the bit detection problem for the uplink, also incorporating the channel estimation error into the analysis. Denote the channel estimation error for the  $k^{\text{th}}$  user by:

$$\tilde{\mathbf{h}}_k = \mathbf{h}_k - \hat{\mathbf{h}}_k. \quad (38)$$

The received signal in (29) can be rewritten as:

$$\mathbf{r} = \sum_{k=1}^K \sqrt{p_k} \hat{\mathbf{h}}_k s_k + \sum_{k=1}^K \sqrt{p_k} \tilde{\mathbf{h}}_k s_k + \mathbf{n}. \quad (39)$$

Since we do not have a closed-form expression for  $\hat{\mathbf{h}}_k$ , the BS may calculate the variance of each realization of  $\tilde{\mathbf{h}}_k$  empirically. From (55), the variance of a complex isotropic Gaussian distribution is 4 times the dispersion parameter.

Heuristically, all channel estimation errors are considered to have a complex isotropic Cauchy distribution. This approach is heuristic because one cannot calculate the variance of the complex Cauchy distribution but our aim is a simple model to find additional dispersion for the noise. Let us denote the dispersion of the  $k^{\text{th}}$  user's channel estimation error by  $\gamma_k$ . Using Proposition 1, the received signal can be expressed as:

$$\mathbf{r} = \sum_{k=1}^K \sqrt{p_k} \hat{\mathbf{h}}_k s_k + \tilde{\mathbf{n}}, \quad (40)$$

where  $\tilde{\mathbf{n}}$  is assumed to be the complex isotropic Cauchy distribution with the dispersion  $\tilde{\gamma} = \sum_{k=1}^K \sqrt{p_k} \gamma_k + \gamma$ . We can replace  $\gamma$  by  $\tilde{\gamma}$  in the conditional probability density functions defined in III-A and IV-B to calculate the uplink BER and the uplink achievable rate.

### D. Soft Decision Metric for The Downlink (Coded Modulation)

For the downlink part, the transmitted signal can be expressed:

$$\mathbf{x} = \mathbf{A} \mathbf{s} = \sum_{k=1}^K \mathbf{a}_k s_k, \quad (41)$$

where  $\mathbf{A}$  is an  $M \times K$  precoder matrix,  $\mathbf{a}_k$  is the  $k^{\text{th}}$  column of  $\mathbf{A}$ , and  $\mathbf{s}$  is an  $K \times 1$  vector including the transmitted symbols. Notice that  $\|\mathbf{a}_k\|_2 = 1$ . The precoder matrix is designed based on the channel estimates. We consider the MR and ZF precoders, for which:

$$\mathbf{A}^{\text{MR}} = \hat{\mathbf{H}}^* \mathbf{D}^{\text{MR}}, \quad (42)$$

$$\mathbf{A}^{\text{ZF}} = \hat{\mathbf{H}}^* (\hat{\mathbf{H}}^T \hat{\mathbf{H}}^*)^{-1} \mathbf{D}^{\text{ZF}}, \quad (43)$$

where  $\mathbf{D}^{\text{MR}}$  and  $\mathbf{D}^{\text{ZF}}$  are  $K \times K$  diagonal matrices for normalization purposes, and the  $k^{\text{th}}$  column of  $\hat{\mathbf{H}}$  is  $\hat{\mathbf{h}}_k$ .

The  $k^{\text{th}}$  user receives the following signal:

$$y_k = \sqrt{p_k} \mathbf{h}_k^T \mathbf{a}_k s_k + \sum_{l=1, l \neq k}^K \sqrt{p_l} \mathbf{h}_k^T \mathbf{a}_l s_l + n_k, \quad (44)$$

where  $p_l^k$  is the received power corresponding to the symbol  $s_l$  at the user  $k$ , and  $n_k$  is the complex isotropic Cauchy noise at the  $k^{\text{th}}$  user.

Note that neither the BS nor the users know the real channels. Moreover, the users do not have access to any channel estimates. Therefore, for the downlink decoding we assume that the  $k^{\text{th}}$  user only knows the corresponding channel gain, which is given by:

$$g_k^{\text{MR}} = \|\hat{\mathbf{h}}_k\|_2, \quad (45)$$

$$g_k^{\text{ZF}} = \mathbf{D}_{kk}^{\text{ZF}}, \quad (46)$$

where  $\mathbf{D}_{kk}^{\text{ZF}}$  refers to the  $k^{\text{th}}$  diagonal element. The LLR expression for the  $i^{\text{th}}$  bit of the  $k^{\text{th}}$  symbol when the MR precoder is used can be expressed as:

$$l_{k,i}^{\text{MR}} = \log \left( \frac{p(b_{k,i} = 0 | y_k)^{\text{MR}}}{p(b_{k,i} = 1 | y_k)^{\text{MR}}} \right) = \log \left( \frac{\sum_{s: b_i(s)=0} p(y_k | s)^{\text{MR}}}{\sum_{s: b_i(s)=1} p(y_k | s)^{\text{MR}}} \right), \quad (47)$$

where  $p(y_k|s)^{\text{MR}}$  is given by:

$$p(y_k|s)^{\text{MR}} = \frac{\gamma}{2\pi \left( \gamma^2 + \left| y_k - \sqrt{p_k^k} g_k^{\text{MR}} s \right|^2 \right)^{3/2}}. \quad (48)$$

To find  $p(y_k|s)^{\text{ZF}}$ , one can replace  $g_k^{\text{MR}}$  by  $g_k^{\text{ZF}}$ .

## V. SIMULATION RESULTS

In this section, we present simulation results. First, we compare the performances of the channel estimates in terms of uncoded SER. Then we present achievable rate results for the perfect and imperfect CSI cases. Finally we present coded BER curves and compare their behavior with the predictions from the achievable rate analysis.

### A. Performances of the Channel Estimates

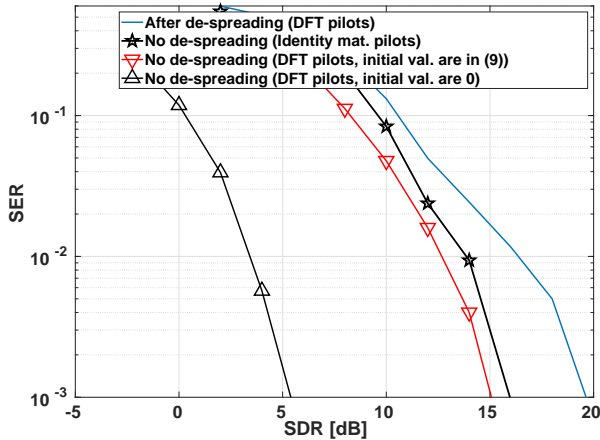


Figure 1. Comparison of the performance of different channel estimation approaches, quantified in terms of (uncoded) SER.

The simulation parameters are as follows: The number of antennas is  $M = 100$ . The number of users and the pilot length are  $K = 8$  and  $\tau = 15$ , respectively. The pilot signals are chosen from the normalized DFT matrix. The channel matrix contains realizations of circularly symmetric Gaussian random variables with unit variance. The dispersion parameter of the Cauchy noise is normalized to unity. We fix the received signal powers of 7 users such that these powers range from 1 to 7 dB. We change the received signal power of the remaining user and observe the effect on the performance. The parameters of the simulation are summarized in Table I.

Table I  
PARAMETERS FOR THE SIMULATIONS

$M$ (number of antennas)	100
$K$ (number of users)	8
$\tau$ (pilot length)	15
$\gamma$ (dispersion parameter)	1
The received signal powers of 7 users [dB]	(1 : 1 : 7)
$T$ for Fig. 1 and Fig. 2 (length of the coherence block)	215
$T$ for all other figures (length of the coherence block)	339
Number of coherence blocks simulated for each SDR	500

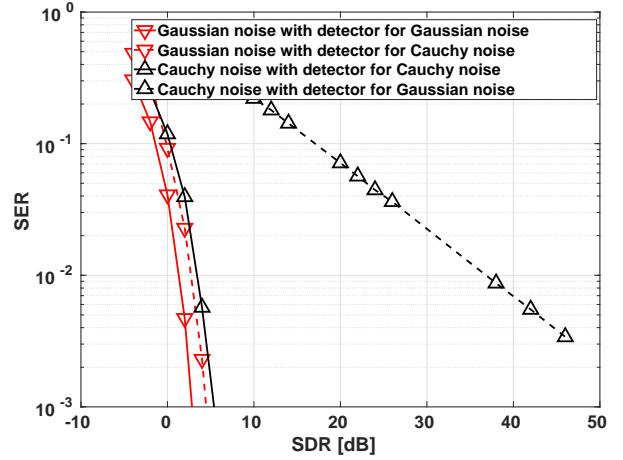


Figure 2. Performances of the detectors in the presence of Cauchy and Gaussian noises, quantified in terms of (uncoded) SER.

We present the effects of the channel estimates on the symbol detection. We have three types of channel estimates: the estimates obtained from the signal after de-spreading, the estimates obtained from the unprocessed signal where the initial values for the algorithm in Section II-B2 are taken from (9), and the estimates obtained from the unprocessed signal where the initial values for the algorithm in Section II-B2 are zero. To generate symbols, each user transmits 200 quadrature-phase-shift keying (QPSK) symbols for each coherence block, whose length is taken to be  $T = 215$ . The small-scale fading for each channel vector is created 500 times so we have  $10^5$  symbols for each SDR.

We present SER performances in Fig. 1. Based on Fig. 1, the detector using the channel estimates obtained from the unprocessed signal outperforms the detector using the channel estimates obtained via the de-spreading operation. One important observation is that the choice of pilot books is important even if the pilot books are chosen from any unitary matrix. For example, based on Fig. 1, if the pilots are chosen from the normalized DFT matrix, we have much better SER performance than the case where the pilots are chosen from the identity matrix. This situation does not appear in the Gaussian noise because the pilot books chosen from any unitary matrix give the same performances [23, Chapter 3]. Therefore, one can conclude that if the noise is Cauchy, one can split the power of the pilots and can increase the number of signal samples in the receiver side. Another important observation is that the channel estimates obtained from the unprocessed signal are sensitive to the initial values used in the algorithm in Section II-B2; this is because the likelihood function of the Cauchy distribution is neither log-concave nor log-convex so it has many local minima. Based on this,  $\hat{\mathbf{h}}_k^{\text{ML}}$  includes outliers causing us to get trapped at poor local optima. Since the mean of the channel realizations is zero, it is expected to obtain a better local optimum point when the initial values are zero.

Quantitatively, when the SER is  $10^{-3}$ , the required SDR for the best detector is almost 5 dB. For SER  $10^{-3}$ , the perfor-



mance gaps to the second and the third detectors compared with the best detector are almost 10 and 15 dB, respectively.

In Fig. 2 we present the performances of two detectors in the presence of two types of noise: Gaussian noise-detector for Gaussian noise, Gaussian noise-detector for Cauchy noise, Cauchy noise-detector for Cauchy noise, and Cauchy noise-detector for Gaussian noise. Note that we change the noise only in the data phase and all detectors use the best channel estimates that are obtained under the Cauchy noise. Based on Fig. 2, the performance gap between the detector for Cauchy and the detector for Gaussian is small in the presence of Gaussian noise. On the other hand, the performance of the detector designed for Gaussian noise is quite poor when the noise is Cauchy. The conclusion is that the detector for Gaussian noise is not robust against the outliers.

For the rest of the paper, we only use the best channel estimates.

### B. Achievable rates with the Cauchy Noise

In this section, we first present the uplink achievable rates of the communication link for both the perfect and imperfect CSI cases. For the modulation scheme, we use QPSK again. The BS has either 100 or 4 antennas and serves a single user. For the imperfect CSI case, the length of the coherence block is  $T = 339$  (we will explain why we choose 339 later).

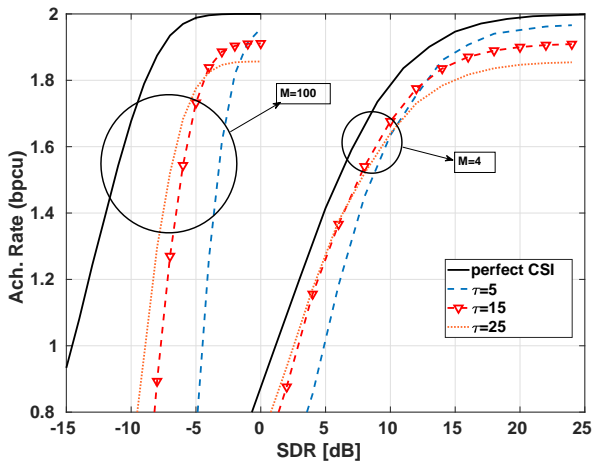


Figure 3. Uplink achievable rates for the perfect and imperfect CSI cases. Here  $\gamma_k$  in the detector is not adjusted to take into account the presence of channel estimation errors.

In Fig. 3, we present uplink performances of the communication link. From Fig. 3, we observe that when we increase the number of antennas we can obtain the same achievable rates with less SDR. For example, when  $\tau$  and the desired rate are chosen to be 15 and 1.8 bits-per-channel-use (bpcu), the required SDR for  $M = 100$  is almost 20 dB less than the required SDR for  $M = 4$ . Another observation is that when we increase the pilot length, we obtain better performances in low SDR. However in high SDR cases, we do not need to use long pilot sequences. Also in any case, we cannot obtain the same performance as in the perfect CSI case, because of the pre-log factors appearing in the achievable rate. In Fig. 4,

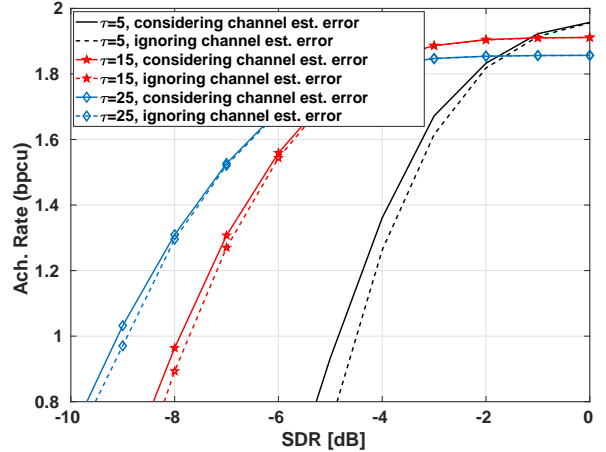


Figure 4. Comparison of uplink achievable rates ( $M = 100$ ) with (“considering”) and without (“ignoring”) adjustment of  $\gamma_k$  to take into account the presence of channel estimation errors, as described in Section IV-C.

we present the uplink achievable rate curves for the two cases that the BS considers the channel estimation error, and ignores it, respectively. We observe that when  $\tau$  increases the gap between two achievable rate curves, i.e., the curve obtained when the BS ignores the channel estimation error and the curve obtained when the BS considers the channel estimation error, gets closer to each other. This result is expected because when  $\tau$  increases, the channel estimation error decreases.

Next, in Fig. 5, we present the downlink achievable rates. Again for the downlink, when we increase the number of antennas, we need less SDR for the same achievable rates and for the low SDR cases we may need longer pilot sequences. Another interesting observation is that the uplink-downlink duality does not hold for the Cauchy noise even for perfect CSI, in contrast to the case of Gaussian noise. With Gaussian noise, when the MR decoder/precoder is used, the structure of the signal is the same both on uplink and downlink. However, this is not the case for the Cauchy noise.

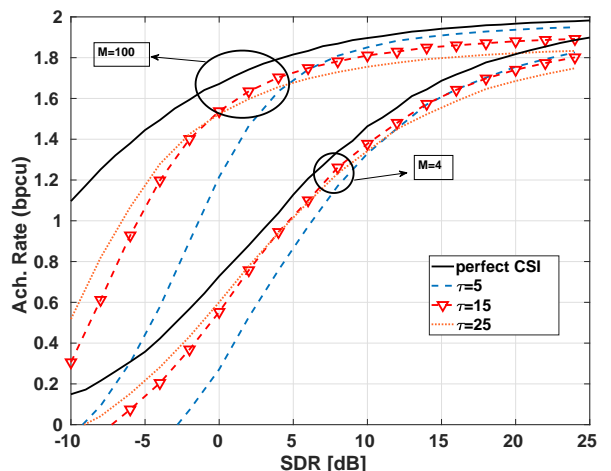


Figure 5. Downlink achievable rates in the perfect and imperfect CSI cases.

Table II  
THE UPLINK BER PERFORMANCES (FIG. 7)

Uplink	The Bounds for Ach. Rate [dB]	Decoding Thr. [dB]	Offset [dB]
$M = 100, K = 1$	-6.4	-5.5	0.9
$M = 100, K = 2$	-6.4	-4.3	2.1
$M = 100, K = 8$	-6.4	1.3	7.7
$M = 4, K = 1$	6.7	9.9	3.2

From Figs. 3 and 5, we do not observe uplink-downlink duality which is consistent with Remark 4 in Section III-B.

In Fig. 6, we present the capacity bound in (26) and the mismatched achievable rate in (28) for QPSK modulation. We generate  $S\alpha S$  noise with unit dispersion for different  $\alpha$ . From Fig. 6, if the noise becomes more impulsive, the gap between the capacity bound and the mismatched achievable rate decreases. Let us focus on code rate  $3/4$ , which corresponds to 1.5 bpcu for QPSK modulation. Numerically, the gaps between these two metrics in (26) and (28) become 3.7, 3.5, 3.1 and 0.9 dB with  $\alpha = 1.8, \alpha = 1.6, \alpha = 1.4$  and  $\alpha = 1.2$ , respectively. In [30], it is shown that the capacity bound becomes tighter for smaller  $\alpha$ . In conclusion, Fig. 6 demonstrates that a decoder metric based on the Cauchy model can perform well in the presence of noise with any  $S(1 < \alpha < 2)S$  distribution.

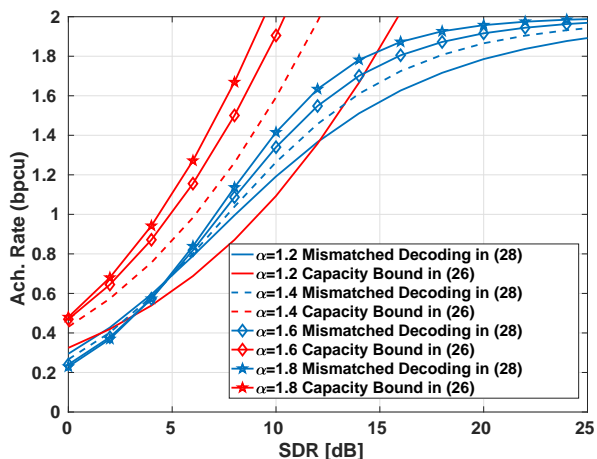


Figure 6.  $S(1 < \alpha < 2)S$  noise vs. Cauchy Decoder: Capacity bounds in (26) and mismatched achievable rate for QPSK in (28) with different  $S\alpha S$  noise.

### C. Coded BER Comparisons

In this section, we present coded BER performance for both the uplink and the downlink. To do this, QPSK modulation is used. For the channel coding, we use a low-density-parity-check (LDPC) code. The coding rate is chosen to be  $3/4$  and there are 648 bits per packet after the encoder. Therefore, the number of transmitted symbols in each packet is 324. We split each packet into 9 sub-packets; each sub-packet occupies 36 symbols in a coherence block and all sub-packets go into different coherence blocks and see different channel realizations. This way, a comparison with the ergodic achievable rates derived in Section III is justified. The length of the pilot vector is 15 in all simulations. We use a coherence block length of

339, which is reasonable for an urban area with some mobility [23].

Note that we divide each coherence block into either a pilot-phase plus an uplink-phase, or into a pilot-phase plus a downlink-phase. For the decoding, we first calculate the LLR values for each bit. These values are then given to the LDPC decoder, which uses belief propagation with 50 iterations.

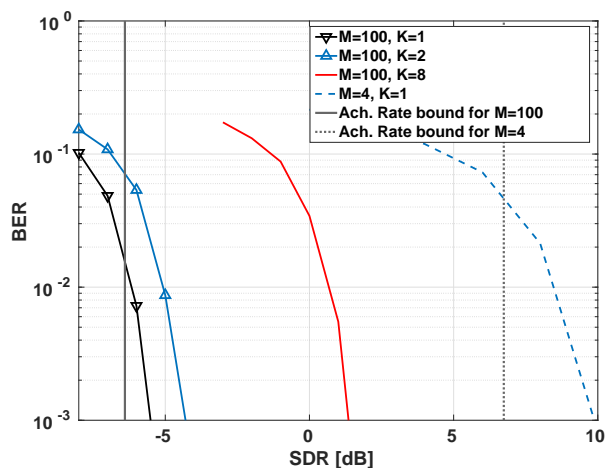


Figure 7. Empirical coded BER for the uplink, without adjusting  $\gamma_k$  in the detector to take into account the presence of channel estimation errors.

First, we consider the uplink performance. Fig. 7 shows the results. For massive MIMO we consider  $K = 1, K = 2$  and  $K = 8$  users. We also present the performance of communication link including a single user ( $K = 1$ ) and a BS ( $M = 4$ ). For the BER curves, the decoding threshold is defined as the SDR value at which the waterfall starts (the SDR value when BER is  $10^{-3}$ ). The quantitative results are presented in Table II. From Fig. 7 and Table II, it is clear that the BER performance gets closer to the achievable rate bound when the number of antennas increases. Note that there is a gap between the decoding threshold obtained from the BER simulations and the bound obtained by the achievable rate analysis. The gap of massive MIMO, ( $M = 100, K = 8$ ), is greater than that of the network, ( $M = 4, K = 1$ ). However, the main advantage is that massive MIMO serves more than one user.

In Fig. 8, we present BER curves for the uplink when the BS considers the channel estimation error in decoding metric. We observe that when the number of users increases, the BER performance improves if the BS considers the channel estimation error. Quantitatively, when the number of users is 8, the BER performance is improved by 0.8 dB. On the other

Table III  
THE DOWNLINK BER PERFORMANCES (FIG. 10)

Downlink	The Bounds for Ach. Rate [dB]	Decoding Thr. [dB]	Offset [dB]
$M = 100, K = 1$	-1.6	2.2	3.8
$M = 100, K = 2$ ZF	-1.6	2.4	4
$M = 100, K = 2$ MR	-1.6	2.6	4.2
$M = 100, K = 8$ ZF	-1.6	5	6.6
$M = 100, K = 8$ MR	-1.6	5.7	7.3
$M = 4, K = 1$	11	15.9	4.9

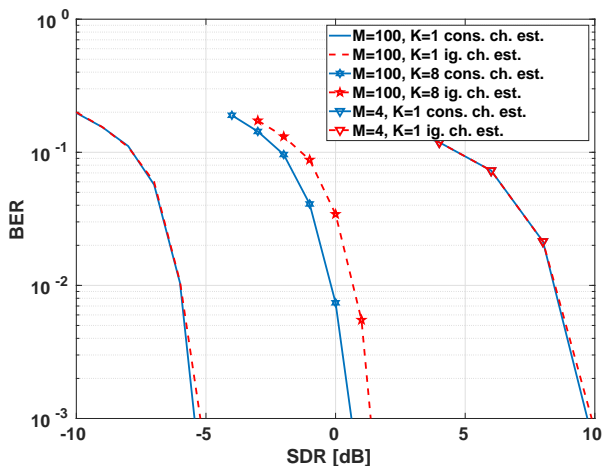


Figure 8. Comparison of coded BER, with (“cons.”) and without (“ig.”) adjustment of  $\gamma_k$  for the presence of channel estimation errors.

hand when the number of user is 1, this improvement becomes 0.2 dB.

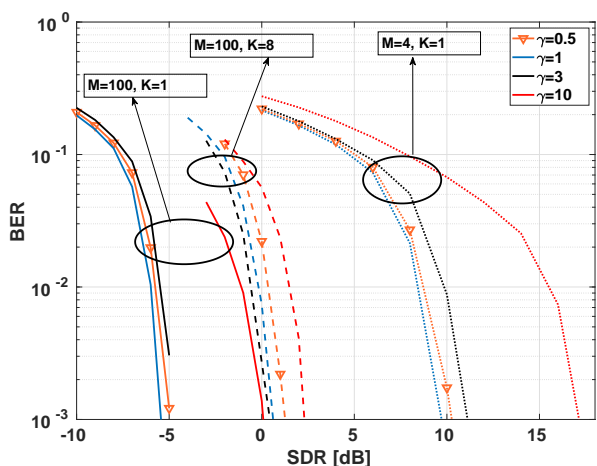


Figure 9. Coded BER curves when the dispersion used in the likelihood function is mismatched to actual real dispersion (the actual dispersion is always 1). All receivers take into account the channel estimation errors.

In Fig. 9, we present the uplink BER curves when the noise dispersions in the likelihood functions are 0.5, 1, 3 and 10 and the dispersion of the noise is 1. When the dispersion in the likelihood function is 0.5 and there is only a single user, we have a relatively low performance loss: around 0.7 dB when  $M = 100$ . Moreover, when  $K = 8$  the receiver whose

dispersion is 3 outperforms the receiver whose dispersion is 1 because of interference.

Similarly, we obtained BER performances for the downlink; see Fig. 10. Compared with the uplink of massive MIMO, we have extra curves corresponding to the two different precoders, MR and ZF. Like for the uplink, in the downlink having more antennas implies that the performance gets closer to the bounds obtained from the achievable rate analysis.

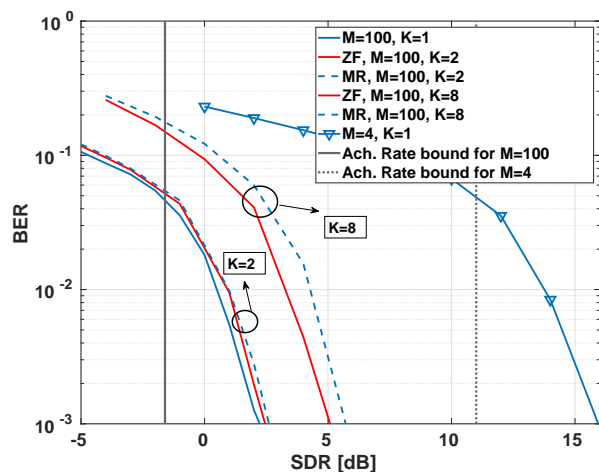


Figure 10. Empirical coded BER for the downlink.

Another observation is that the ZF precoder performs slightly better than the MR precoder when the number of users is 8. These precoders perform almost the same when the number of users is 2. This is expected because the user-interference is so small when there are 2 users so these precoders are almost identical. The numerical results are presented in Table III.

## VI. CONCLUSIONS

We investigated massive MIMO with Cauchy noise from three perspectives: channel estimation, achievable rates and soft bit detection. First, we obtained the channel estimates from uplink pilots in two ways: with and without de-spreading the received pilot signal. In contrast to the case of Gaussian noise, with Cauchy noise the de-spreading operation does not result in a sufficient statistic for the channel estimation. Consequently, better channel estimation performance is obtained when using the unprocessed received signal.

Next, we obtained uplink and downlink achievable rates for the cases of perfect and imperfect CSI (using the channel estimates we developed). We observed that for low SDR,

longer pilot signals can be used to obtain better achievable rates. Also, the achievable rate increases with an increasing number of antennas on both uplink and downlink. We also compared the performance of Cauchy decoding with a capacity bound for general S $\alpha$ S noise available in the literature. Through simulations, we validated the technical soundness of using the Cauchy receiver for other S $\alpha$ S noise.

We compared the detectors designed for the Cauchy and Gaussian noises in the presence of both types of noises. An important observation is that the performance losses both of the detector designed for Cauchy noise and of the detector designed for Gaussian noise are small in the presence of Gaussian noise. However, the detector designed for Gaussian noise works poorly in the presence of Cauchy noise. This means that unlike the Gaussian-noise detector, the Cauchy-noise detector is very robust, and should be a preferred choice whenever robustness to unknown noise distributions is a priority.

Finally, we obtained metrics for soft bit detection. Based on these metrics, we performed numerical simulations of the BER, using LDPC coding and QPSK modulation. We compared the threshold of this BER performance with the achievable rate bound. The main conclusions are that the gap between the decoding threshold and achievable rate bound is small, and that this gap decreases with an increasing number of antennas.

#### APPENDIX A MATHEMATICAL PRELIMINARIES

A real-valued random variable S $\alpha$ S is defined by its characteristic function [37]:

$$\phi(t) = \exp(j\delta t - \gamma|t|^\alpha), \quad (49)$$

where  $t \in \mathbb{R}$ ,  $\delta$  is the location parameter,  $\gamma$  is the dispersion parameter which determines the spread of the distribution in  $\gamma > 0$ , and  $\alpha$  is the characteristic exponent which satisfies  $0 < \alpha \leq 2$  and determines the tail level of distribution. A smaller  $\alpha$  yields a more impulsive and heavily-tailed distribution, and vice versa. There are two important special cases of the S $\alpha$ S distribution: Cauchy ( $\alpha = 1$ ) and Gaussian ( $\alpha = 2$ ), which both have pdfs in closed form. These pdfs, if  $\delta = 0$ , are given by

$$c(x) = \frac{\gamma}{\pi(x^2 + \gamma^2)}, \quad (50)$$

for the Cauchy case and

$$g(x) = \frac{1}{\sqrt{4\pi\gamma}} \exp\left(-\frac{x^2}{4\gamma}\right), \quad (51)$$

for the Gaussian. From (50) and (51), two important results can be obtained: For the Gaussian distribution, the variance is  $2\gamma$ . For the Cauchy distribution, the mean and variance are undefined. More precisely the variance is infinite because  $\mathbb{E}[|\mathbf{X}|^p] = \infty$  if  $p \geq \alpha$ .

In communication problems, we generally deal with complex-valued random variables. Define the complex Cauchy random variable  $X = X^R + jX^I$  where  $X^R$  and  $X^I$  are jointly S( $\alpha = 1$ )S. By definition, the characteristic function is:

$$\phi_X(\omega) = \mathbb{E}[\exp(j\Re(\omega X^*))], \quad (52)$$

where  $\omega \in \mathbb{C}$ .  $X$  is an isotropic complex Cauchy random variable if and only if the characteristic function has the form [33, Chapter 3]:

$$\phi_X(\omega) = \exp(-\gamma|\omega|). \quad (53)$$

The pdf of an isotropic complex Cauchy distribution is:

$$f_X(x) = \frac{\gamma}{2\pi(|x|^2 + \gamma^2)^{3/2}}. \quad (54)$$

As the name ‘‘isotropic’’ suggests, the pdf is invariant to a rotation of the complex angle and depends only on the magnitude of the realization from (54). The marginal distributions of  $X^R$  and  $X^I$  can be easily obtained and they are same as for the pdf in (50). An important property of the isotropic complex Cauchy distribution is that  $X^R$  and  $X^I$  are statistically dependent. This can be immediately seen from the fact that the product of the pdfs of  $X^R$  and  $X^I$  is not equal to the joint pdf in (54). This is a fundamental difference between the isotropic complex Cauchy and isotropic complex Gaussian distributions. (For the latter, in-phase and quadrature components are independent, which is also referred to as circular symmetry of the noise [38, Chapter 3].) For the sake of completeness, the pdf of an isotropic complex Gaussian random variable,  $Y$ , (which necessarily has zero mean) is given by:

$$f_Y(x) = \frac{1}{4\pi\gamma} \exp\left(-\frac{|x|^2}{4\gamma}\right). \quad (55)$$

#### APPENDIX B

##### SOLVING THE OPTIMIZATION PROBLEM IN (14)

We denote the objective function in (14) by  $f$ . We use the gradient descent algorithm [26, Chapter 3]. The optimization variables are  $\mathbf{h}_1^R[1]$  and  $\mathbf{h}_1^I[1]$ , corresponding to the real and imaginary parts of  $\mathbf{h}_1[1]$ . Before defining the gradient vector, let us define the following auxiliary functions:

$$p(\mathbf{h}_1^R[1], \mathbf{h}_1^I[1], i) = \mathbf{Y}'^R[1, i] - \sqrt{\tau p_1} \left( \mathbf{h}_1^R[1] \phi_1^R[i] - \mathbf{h}_1^I[1] \phi_1^I[i] \right), \quad (56)$$

$$r(\mathbf{h}_1^R[1], \mathbf{h}_1^I[1], i) = \mathbf{Y}'^I[1, i] - \sqrt{\tau p_1} \left( \mathbf{h}_1^I[1] \phi_1^R[i] + \mathbf{h}_1^R[1] \phi_1^I[i] \right). \quad (57)$$

The gradient of the objective function in (14) can now be expressed as:

$$\nabla f \begin{bmatrix} \mathbf{h}_1^R[1] \\ \mathbf{h}_1^I[1] \end{bmatrix} = -2\sqrt{\tau p_1} \times \begin{bmatrix} \sum_{i=1}^{\tau} \frac{\phi_1^R[i] p(\mathbf{h}_1^R[1], \mathbf{h}_1^I[1], i) + \phi_1^I[i] r(\mathbf{h}_1^R[1], \mathbf{h}_1^I[1], i)}{\gamma^2 + |\mathbf{Y}'[1, i] - \sqrt{\tau p_1} \mathbf{h}_1[1] \phi_1[i]|^2} \\ \sum_{i=1}^{\tau} \frac{-\phi_1^I[i] p(\mathbf{h}_1^R[1], \mathbf{h}_1^I[1], i) + \phi_1^R[i] r(\mathbf{h}_1^R[1], \mathbf{h}_1^I[1], i)}{\gamma^2 + |\mathbf{Y}'[1, i] - \sqrt{\tau p_1} \mathbf{h}_1[1] \phi_1[i]|^2} \end{bmatrix}. \quad (58)$$

With the gradient descent approach, we update the channel vector according to:

$$\begin{bmatrix} \mathbf{h}_1^R[1] \\ \mathbf{h}_1^I[1] \end{bmatrix}^{j+1} = \begin{bmatrix} \mathbf{h}_1^R[1] \\ \mathbf{h}_1^I[1] \end{bmatrix}^j - \eta_j \nabla f \left( \begin{bmatrix} \mathbf{h}_1^R[1] \\ \mathbf{h}_1^I[1] \end{bmatrix}^j \right). \quad (59)$$

where  $\begin{bmatrix} \mathbf{h}_1^R[1] \\ \mathbf{h}_1^I[1] \end{bmatrix}^j$  and  $\eta_j$  are the vectors that represent the solutions and the step length for the  $j^{\text{th}}$  iteration, respectively.  $\eta_j$  can be chosen differently for each iteration using, for example, the backtracking algorithm [26, Chapter 3]. Note that the cost of obtaining the gradient for one channel realization is  $\mathcal{O}(\tau)$  flops, and for all channel realizations the cost is  $\mathcal{O}(MK\tau)$  flops.

## APPENDIX C

### EMPIRICAL CALCULATION OF SISO CHANNEL'S MUTUAL INFORMATION

The mutual information between channel input  $X$ , and channel output  $Y$  can be defined as:

$$I(X; Y) = H(X) - H(X|Y). \quad (60)$$

Let us assume that  $X$  is chosen uniformly from a certain discrete set  $A_X$  with cardinality  $S$ . Then, (60) can be written as:

$$I(X; Y) = \log_2 S - \int \sum_{x \in A_X} -p(x, y) \log_2(p(x|y)) dy, \quad (61)$$

where  $p(x, y)$  is the joint probability density function of  $X$  and  $Y$ , and  $p(x|y)$  is the conditional probability density function. The second term is the expectation of  $(-\log_2(p(x|y)))$  with respect to  $X$  and  $Y$ . By using Bayes' rule, we can re-write mutual expression as:

$$\begin{aligned} I(X; Y) &= \log_2 S - \mathbb{E}_{X, Y} \left\{ \log_2 \frac{p(Y)}{p(X, Y)} \right\}, \quad (62) \\ &= \log_2 S - \mathbb{E}_{X, Y} \left\{ \log_2 \frac{\sum_{x \in A_X} p(Y|x)p(x)}{p(Y|X)p(X)} \right\}, \\ &= \log_2 S - \mathbb{E}_{X, Y} \left\{ \log_2 \frac{\sum_{x \in A_X} p(Y|x)}{p(Y|X)} \right\}. \end{aligned}$$

Now, we consider a perfect CSI case where the receiver has the perfect knowledge of channel. The mutual information is given [31]:

$$I(X; Y|H) = H(X|H) - H(X|H, Y). \quad (63)$$

Note that  $X$  is independent of  $H$ . By following the steps in (62), (63) can be rewritten as:

$$I(X; Y|H) = \log_2 S - \mathbb{E}_{X, Y, H} \left\{ \log_2 \frac{\sum_{x \in A_X} p(Y|H, x)}{p(Y|H, X)} \right\}. \quad (64)$$

The expectation terms in (62) and (64) can be calculated by Monte Carlo simulations.

## REFERENCES

- [1] Z. Gülgün and E. G. Larsson, "Channel Estimation for Massive MIMO in the Presence of Cauchy Noise," in *IEEE International Conference on Communications (ICC)*, 2022, pp. 1769–1774.
- [2] E. Björnson, L. Sanguinetti, H. Wymeersch, J. Hoydis, and T. L. Marzetta, "Massive MIMO is a Reality—What is Next?: Five Promising Research Directions for Antenna Arrays," *Digital Signal Processing*, vol. 94, pp. 3–20, 2019, special Issue on Source Localization in Massive MIMO.
- [3] T. Van Chien, E. Björnson, and E. G. Larsson, "Joint Power Allocation and User Association Optimization for Massive MIMO Systems," *IEEE Trans. Wireless Commun.*, vol. 15, no. 9, pp. 6384–6399, 2016.
- [4] C. Mollén, U. Gustavsson, T. Eriksson, and E. G. Larsson, "Spatial Characteristics of Distortion Radiated From Antenna Arrays With Transceiver Nonlinearities," *IEEE Trans. Wireless Commun.*, vol. 17, no. 10, pp. 6663–6679, 2018.
- [5] M. Matthaiou, O. Yurduseven, H. Q. Ngo, D. Morales-Jimenez, S. L. Cotton, and V. F. Fusco, "The Road to 6G: Ten Physical Layer Challenges for Communications Engineers," *IEEE Commun. Mag.*, vol. 59, no. 1, pp. 64–69, 2021.
- [6] E. Axell, P. Eliardsson, S. Tengstrand, and K. Wiklundh, "Power Control in Interference Channels With Class A Impulse Noise," *IEEE Wireless Commun. Lett.*, vol. 6, no. 1, pp. 102–105, 2017.
- [7] J. Zhang, L. Liu, K. Wang, Y. Fan, and J. Qiu, "Measurements and Statistical Analyses of Electromagnetic Noise for Industrial Wireless Communications," *Int. J. of Intell. Syst.*, vol. 36, no. 3, pp. 1304–1330, 2021.
- [8] J. Ferrer-Coll, S. Slimane, J. Chilo, and P. Stenumgaard, "Detection and Suppression of Impulsive Noise in OFDM Receiver," *Wireless Pers. Commun.*, vol. 85, p. 2245–2259, 2015.
- [9] Q. Zheng, F. Wang, B. Ai, and Z. Zhong, "Multicarrier Downlink Transmission for High-speed Railway in Non-Gaussian Noise Channels," *IEEE Access*, vol. 6, pp. 52 607–52 615, 2018.
- [10] J. Ferrer-Coll, B. Slimane, J. Chilo, and P. Stenumgaard, "Impulsive noise detection in OFDM systems with PAPR reduction," in *2014 International Symposium on Electromagnetic Compatibility*, 2014, pp. 523–527.
- [11] K. Häggglund and E. Axell, "Adaptive Demodulation in Impulse Noise Channels," *IEEE Trans. Veh. Tech.*, vol. 71, no. 2, pp. 1685–1698, 2022.
- [12] M. Chitre, J. Potter, and S.-H. Ong, "Optimal and Near-Optimal Signal Detection in Snapping Shrimp Dominated Ambient Noise," *IEEE J. Ocean. Eng.*, vol. 31, no. 2, pp. 497–503, 2006.
- [13] M. Zimmermann and K. Dostert, "Analysis and Modeling of Impulsive Noise in Broad-band Powerline Communications," *IEEE Trans. Electromag. Compat.*, vol. 44, no. 1, pp. 249–258, 2002.
- [14] E. Sousa, "Performance of A Spread Spectrum Packet Radio Network Link in A Poisson Field of Interferers," *IEEE Trans. Inf. Theory*, vol. 38, no. 6, pp. 1743–1754, 1992.
- [15] S. R. K. Vadali, P. Ray, S. Mula, and P. K. Varshney, "Linear Detection of a Weak Signal in Additive Cauchy Noise," *IEEE Trans. on Commun.*, vol. 65, no. 3, pp. 1061–1076, 2017.
- [16] P. Tsakalides and C. Nikias, "The Robust Covariation-based MUSIC (ROC-MUSIC) Algorithm for Bearing Estimation in Impulsive Noise Environments," *IEEE Trans. Signal Process.*, vol. 44, no. 7, pp. 1623–1633, 1996.
- [17] —, "Robust Adaptive Beamforming in Alpha-stable Noise Environments," in *1996 IEEE International Conference on Acoustics, Speech, and Signal Processing Conference Proceedings*, vol. 5, 1996, pp. 2884–2887 vol. 5.
- [18] M. Liu, N. Zhao, J. Li, and V. C. M. Leung, "Spectrum Sensing Based on Maximum Generalized Correntropy Under Symmetric Alpha Stable Noise," *IEEE Trans. Veh. Tech.*, vol. 68, no. 10, pp. 10 262–10 266, 2019.
- [19] P. Tsakalides and C. Nikias, "Maximum Likelihood Localization of Sources in Noise Modeled as A Stable Process," *IEEE Trans. Signal Process.*, vol. 43, no. 11, pp. 2700–2713, 1995.
- [20] Y. Chen and J. Chen, "Novel S $\alpha$ S PDF Approximations and Their Applications in Wireless Signal Detection," *IEEE Trans. Wireless Commun.*, vol. 14, no. 2, pp. 1080–1091, 2015.
- [21] M. R. Souryal, E. G. Larsson, B. Peric, and B. R. Vojcic, "Soft-Decision Metrics for Coded Orthogonal Signaling in Symmetric Alpha-Stable Noise," *IEEE Trans. Signal Process.*, vol. 56, no. 1, pp. 266–273, 2008.
- [22] L. Zhou, J. Dai, W. Xu, and C. Chang, "Uplink Channel Estimation for Massive MIMO Systems With Impulsive Noise," *IEEE Commun. Lett.*, vol. 25, no. 5, pp. 1534–1538, 2021.
- [23] T. L. Marzetta, E. G. Larsson, H. Yang, and H. Q. Ngo, *Fundamentals of Massive MIMO*. Cambridge University Press, 2016.
- [24] E. Björnson, J. Hoydis, and L. Sanguinetti, "Massive MIMO Networks: Spectral, Energy, and Hardware Efficiency," *Foundations and Trends® in Signal Processing*, vol. 11, no. 3–4, pp. 154–655, 2017.
- [25] S. M. Kay, *Fundamentals of Statistical Signal Processing: Estimation Theory*. Upper Saddle River, NJ, USA: Prentice-Hall, Inc., 1993.
- [26] J. Nocedal and S. Wright, *Numerical Optimization*, ser. Springer Series in Operations Research and Financial Engineering. Springer New York, 2006.
- [27] M. J. D. Powell, "On search directions for minimization algorithms," *Mathematical Programming*, vol. 4, pp. 193–201, 1973.
- [28] D. Bertsekas, *Nonlinear Programming*, ser. Athena scientific optimization and computation series. Athena Scientific, 2016.

- [29] J. Fahs and I. Abou-Faycal, "A Cauchy Input Achieves The Capacity of a Cauchy Channel Under A Logarithmic Constraint," in *2014 IEEE International Symposium on Information Theory*, 2014, pp. 3077–3081.
- [30] M. L. de Freitas, M. Egan, L. Clavier, A. Goupil, G. W. Peters, and N. Azaoui, "Capacity Bounds for Additive Symmetric  $\alpha$ -Stable Noise Channels," *IEEE Trans. Inf. Theory*, vol. 63, no. 8, pp. 5115–5123, 2017.
- [31] M. Medard, "The Effect upon Channel Capacity in Wireless Communications of Perfect and Imperfect Knowledge of The Channel," *IEEE Trans. Inf. Theory*, vol. 46, no. 3, pp. 933–946, 2000.
- [32] D. Tse and P. Viswanath, *Fundamentals of Wireless Communication*. Cambridge University Press, 2005.
- [33] P. Tsakalides, "Array signal processing with alpha-stable distributions," Ph.D. dissertation, Univ. Southern California, Los Angeles, CA, 1995.
- [34] N. Merhav, G. Kaplan, A. Lapidoth, and S. Shamai Shitz, "On information rates for mismatched decoders," *IEEE Trans. Inf. Theory*, vol. 40, no. 6, pp. 1953–1967, 1994.
- [35] D. Arnold, H. A. Loeliger, P. Vontobel, A. Kavcic, and W. Zeng, "Simulation-Based Computation of Information Rates for Channels With Memory," *IEEE Trans. Inf. Theory*, vol. 52, no. 8, pp. 3498–3508, 2006.
- [36] E. G. Larsson and J. Jalden, "Fixed-Complexity Soft MIMO Detection via Partial Marginalization," *IEEE Trans. Signal Process.*, vol. 56, no. 8, pp. 3397–3407, 2008.
- [37] M. Shao and C. Nikias, "Signal Processing with Fractional Lower Order Moments: Stable Processes and Their Applications," *Proceedings of the IEEE*, vol. 81, no. 7, pp. 986–1010, 1993.
- [38] R. Gallager, *Stochastic Processes: Theory for Applications*. Cambridge University Press, 2013.